
Regularizing and Aggregating Clients with Class Distribution for Personalized Federated Learning

Gyujeong Lee

SAKAK Inc.
Seoul, Republic of Korea, 04147
regulation.lee@sakak.co.kr

Daeyeung Choi

The Cyber University of Korea
Seoul, Republic of Korea, 03051
choidy@cuk.edu

Abstract

Personalized federated learning (PFL) enables customized models for clients with varying data distributions. However, existing PFL methods often incur high computational and communication costs, limiting their practical application. This paper proposes a novel PFL method, Class-wise Federated Averaging ($cwFedAVG$), that performs Federated Averaging ($FedAVG$) class-wise, creating multiple global models per class on the server. Each local model integrates these global models weighted by its estimated local class distribution, derived from the L2-norms of deep network weights, avoiding privacy violations. Afterward, each global model does the same with local models using the same method. We also newly designed Weight Distribution Regularizer (WDR) to further enhance the accuracy of estimating a local class distribution by minimizing the Euclidean distance between the class distribution and the weight norms' distribution. Experimental results demonstrate that $cwFedAVG$ matches or outperforms several existing PFL methods. Notably, $cwFedAVG$ is conceptually simple yet computationally efficient as it mitigates the need for extensive calculation to collaborate between clients by leveraging shared global models. Visualizations provide insights into how $cwFedAVG$ enables local model specialization on respective class distributions while global models capture class-relevant information across clients.

1 Introduction

Federated learning (FL) enables client collaboration by aggregating locally-trained models (McMahan et al., 2017; Kairouz et al., 2021). Typically, one global model in the server exists, but creating a single global model without considering data heterogeneity across clients can lead to poor performance for each client and non-guaranteed convergence when client data is non-IID (non-independent and identically distributed) (Zhao et al., 2018; Li et al., 2020; Hsieh et al., 2020). To address this problem, various personalized federated learning (PFL) methods have emerged that aim to learn personalized models tailored to individual clients.

PFL can be categorized into two main approaches: global model personalization and learning individualized models (Tan et al., 2022). The first approach involves two steps: 1) training a single global model and 2) personalizing the trained global model for each FL client through a local adaptation step that involves additional training on each local dataset (Fallah, Mokhtari, and Ozdaglar, 2020; Collins et al., 2021). The second approach trains separate personalized models for each client from the outset by modifying how the models are aggregated during the federated learning process to create customized models for each client. The second approach has an advantage over the first because it seeks to encapsulate the relevant information within the global model by employing a personalized aggregation (Zhang et al., 2023a).

In this paper, we explore the second approach, which, albeit promising, still faces several challenges. Firstly, in personalized aggregation-based methods, clients often require substantial memory or

computational resources to acquire relevant information from other clients. This information exchange can be facilitated by combining weighted local models (Luo and Wu, 2022; Zhang et al., 2020) and pairwise collaboration among clients (Huang et al., 2021). Secondly, clustering-based methods can mitigate the first challenge by partitioning clients into groups based on gradients or losses and performing FL within each group (Sattler, Müller, and Samek, 2020; Ghosh et al., 2020; Briggs, Fan, and Andras, 2020; Duan et al., 2021). However, the assumption that a few discrete groups can exist is often considered too strong, and the computation cost for clustering remains high.

To address these challenges, we introduce a novel PFL method, Class-wise Federated Averaging ($cwFedAVG$). This method performs Federated Averaging ($FedAVG$) class-wise, creating multiple global models (referred to as ‘class-specific global model’ in this study) on the server, each corresponding to a class. Each class-specific global model aggregates local models weighted by the proportion of that class’s data in its local dataset. Subsequently, each local model aggregates the global models weighted by the proportion of that class’s data in its local dataset. This method is based on the assumption that the weights of a local model encapsulate class-specific information proportional to the class distribution in the local dataset, as the model’s weight updates are driven by the distribution.

For performing $cwFedAVG$, the server requires knowledge of the class distribution of each client’s dataset. However, explicitly transmitting this distribution to the server can violate privacy constraints. Consequently, we introduce a proxy method to estimate the class distribution of a client from the deep network weights. This method computes the L2-norms of the weights connecting the penultimate layer to each output neuron, as they are correlated with the client’s class distribution. However, this correlation is insufficient for accurate class distribution estimation. To further enhance the accuracy of class distribution estimation, we newly designed and applied Weight Distribution Regularizer (WDR) that minimizes the distance between the norms’ distribution and class distribution.

The empirical evaluation demonstrates that $cwFedAVG$, when coupled with WDR , achieves comparable performance to several PFL methods across four benchmark datasets with non-IID data partitions. Furthermore, the visualizations of the L2-norms of the weight vectors provide compelling evidence that $cwFedAVG$ with WDR enables effective personalization of local models.

Our contributions can be summarized as follows.

- We introduce a novel method called $cwFedAVG$ for PFL. Our method, while being conceptually simple, is also computationally efficient. Importantly, our experimental results show that $cwFedAVG$ with WDR outperforms or performs comparably to several existing PFL methods.
- Additionally, we introduce a new proxy method that estimates the client’s class distribution using the weights of a deep network. It is advantageous over other methods because it does not rely on an auxiliary dataset for estimation. Moreover, we design a novel regularizer, WDR that significantly enhances the accuracy of class distribution estimation by regularizing deep network weights, thus improving the performance of $cwFedAVG$.
- Finally, through visualizations of the norms of deep network’s weight vectors, we provide insights into the personalization of models. Specifically, these visualizations reveal that each local model is tailored to perform well on the local dataset’s class distribution, and each global model effectively captures information relevant to that class when $cwFedAVG$ is used.

2 Related Work

Personalized Federated Learning Among various PFL approaches, our work relates to several recent methods that create customized models for each client by applying modified aggregation techniques. $FedFomo$ (Zhang et al., 2020) encourages FL among only relevant clients by utilizing an optimally weighted combination of models from those clients. $FedAMP$ (Huang et al., 2021) is an attention-based technique that promotes stronger collaborative interactions between clients with comparable data distributions. $APPLE$ (Luo and Wu, 2022) aggregates client models locally with adaptively learned weights, representing the extent of client collaboration. While effective, these methods often require heavy computation to learn the weights or communication to download other clients’ models. Clustering-based FL methods can mitigate this issue by performing FL in each client cluster. CFL (Sattler, Müller, and Samek, 2020) utilizes hierarchical clustering with a cosine similarity of clients’ gradient updates as a post-processing step of FL. $IFCA$ (Ghosh et al., 2020) assigns clients

to one of the pre-determined K clusters and performs model aggregation within each cluster on the server. Briggs, Fan, and Andras (2020) adds a hierarchical clustering step to the FL step for separating client clusters according to the similarity of clients’ model weight updates. Long et al. (2023) groups clients based on the parameters of their models. It learns multiple global models, serving as the cluster centers, and determines the assignment of clients to the centers. Akin to the listed approaches, our `cwFedAVG` method leverages relevant clients to personalize local models. However, it distinguishes itself by circumventing the need to learn weights governing client collaboration and does not require strong assumptions for clustering clients that clients can be partitioned into multiple discrete groups.

Estimating Class Distribution from a Deep Network In centralized machine learning, utilizing class distribution information for classification is often considered crucial, as a class imbalance can adversely impact generalization performance (Johnson and Khoshgoftaar, 2019; Choi and Rhee, 2019). Numerous techniques have been proposed to mitigate this performance degradation in class-imbalanced learning. Notably, Anand et al. (1993) revealed a correlation between the number of data samples for each class and the magnitude of gradients associated with that class. They proposed an algorithm to accelerate learning by exploiting this correlation. In the realm of FL, utilizing class distribution is pivotal as it can be employed for client selection Yang et al. (2021) on the server and loss function modification (Wang et al., 2021; Zhang et al., 2022) on clients. However, due to privacy concerns, directly transmitting class distribution information from clients to the server is typically prohibited. Consequently, several proxy methods have been proposed to estimate class distribution from a deep network. Yang et al. (2021) utilized the gradient magnitude as a proxy to estimate the class distributions of clients and employed it for client selection. Wang et al. (2021) developed a monitoring scheme that estimates class distribution based on the work of Anand et al. (1993). Our class distribution estimation method was motivated by Anand et al. (1993). However, we instead use the weights of a deep network, not gradients. Moreover, we enhanced the method by applying WDR to strengthen the correlation between class distribution and weight distribution.

3 Class-wise Federated Averaging for Personalized Federated Learning

In this section, we first assume the server can access all clients’ class distribution information, and based on this assumption, we explain `cwFedAVG` in detail.

Problem Formulation and Notation FL enhances the performance of individual models by updating the global model with the aggregation of individual models’ parameters without sharing data, thus preserving privacy. Its objective can be summarized as follows.

$$\min_{\mathbf{w}} f_G(\mathbf{w}) = \min_{\mathbf{w}} \sum_{i=1}^M p_i F_i(\mathbf{w}), \quad (1)$$

where $f_G(\cdot)$ and $F_i(\cdot)$ denote the global objective and the local objective of client i , respectively. The global objective $f_G(\mathbf{w})$ is the weighted sum of M local objectives, with M being the number of clients. The weight p_i for each client is defined as the ratio of the number of data samples n_i on that client to the total number of data samples $n = \sum_{i=1}^M n_i$ across all clients, thus $p_i = \frac{n_i}{n}$. The local objective $F_i(\cdot)$ for each client i can be defined as the expected loss over the data distribution \mathcal{D}_i specific to that client. However, since we only have access to a finite set of data points, we approximate this expected loss using the empirical risk calculated over the local training data \mathcal{D}_i^{tr} available to the client. This empirical risk minimization is expressed as $\mathbb{E}_{z \sim \mathcal{D}_i} [\mathcal{L}(\cdot; z)] \approx \frac{1}{n_i} \sum_{z \in \mathcal{D}_i^{tr}} \mathcal{L}(\cdot; z)$, where z represents the data under local distribution \mathcal{D}_i . In PFL, the global objective can take a more flexible form. Instead of a single global model, the goal is to optimize a set of personalized models, one for each client. This can be expressed as (Luo and Wu, 2022):

$$\min_{\mathbf{W}} f_P(\mathbf{W}) = \min_{\mathbf{w}_i, i \in [M]} f_P(\mathbf{w}_1, \dots, \mathbf{w}_M), \quad (2)$$

where $f_P(\mathbf{W})$ is the global objective for the PFL algorithm, and \mathbf{W} is a matrix containing all the personalized models, $\mathbf{W} = [\mathbf{w}_1, \mathbf{w}_2, \dots, \mathbf{w}_M]$. The goal is to find the optimal set of personalized models \mathbf{W}^* that minimizes the global objective function $f_P(\mathbf{W})$. This optimal set \mathbf{W}^* is equivalently represented by the optimal individual personalized models \mathbf{w}_i^* , where i ranges from 1 to M .

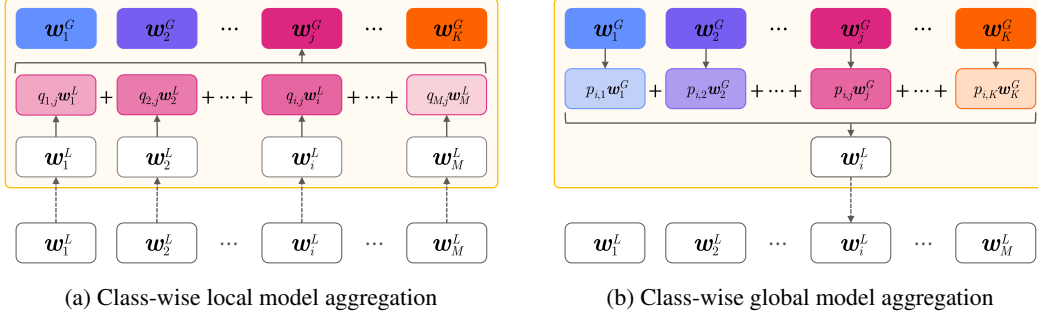


Figure 1: Aggregation process of cwFedAVG . The different colors represent different class-specific global models, and the darker the color, the higher the weight applied during aggregation. The yellow shaded area represents the server.

3.1 Class-wise Local Model Aggregation

cwFedAVG consists of two model aggregation stages, unlike FedAVG , which only has a local model aggregation. FedAVG updates the single global model by iteratively averaging the updates of local models in each round, a process known as ‘local model aggregation’. We extend this to ‘class-wise local model aggregation.’ Assuming the server knows each client’s class distribution, a client’s local model can be decomposed into a set of weighted models, with one model per class. Formally, the weighted local model for class j on client i can be represented as $w_{i,j}^L = p_{i,j}w_i^L$, where w_i^L denotes the local model for client i , and $p_{i,j} = \frac{n_{i,j}}{n_i}$ is the ratio of the number of data samples belonging to class j on client i to the total number of data samples possessed by that client. (This paper uses the indices i and j to represent individual clients (or local models) and distinct classes (or global models), respectively.) With the weighted models, the server performs Federated Averaging class-wise across all clients as shown in Figure 1a. Formally, the class-specific global model for class j can be represented as follows.

$$w_j^G = \sum_{i=1}^M q_{i,j} w_i^L \quad (3)$$

$$= \sum_{i=1}^M \frac{p_i \cdot p_{i,j}}{\sum_{i=1}^M p_i \cdot p_{i,j}} w_i^L \quad (4)$$

$$= \sum_{i=1}^M \frac{n_{i,j}}{\sum_{i=1}^M n_{i,j}} w_i^L, \quad (5)$$

where $q_{i,j}$ is a normalization factor representing the ratio of the number of j -th class’ data samples on client i and the number of j -th class’ data samples across all clients. Therefore, from Eq. (5), we can observe that the class-wise local model aggregation is analogous to the aggregation of FedAVG , except that it is performed class-wise with class-specific global models and a different normalization factor, which involves only the data samples of the j -th class. Complete derivation for the normalization term can be found in the supplementary materials. Now, we derive the relationship between FedAVG and cwFedAVG under the assumption about specific data distribution across the clients.

Theorem 1. *Let w_j^G and w^G be any j -th class-specific global model learned by cwFedAVG and the global model learned by FedAVG , respectively. Then*

$$w_j^G = w^G \quad (6)$$

if all clients have the complete set of classes in their local datasets, and the class distribution is uniform in each client.

Theorem 1 can be easily proved by the fact that $p_{i,j} = \frac{1}{K}$ for any client i with Eq. (4). The proof of the theorem is provided in the supplementary materials.

3.2 Class-wise Global Model Aggregation

In contrast to FedAVG, where a single global model is copied to each local model, cwFedAVG performs a weighted summation of class-specific global models to update each local model. Specifically, for the i -th local model, its update from the j -th class-specific global model is weighted by the ratio of data belonging to class j in the local dataset, thus $\mathbf{w}_{j,i}^G = p_{i,j} \mathbf{w}_j^G$. The server sums up all the weighted class-specific global models from K classes to update the i -th local model, as shown in Figure 1b and the following equation:

$$\mathbf{w}_i^L = \sum_{j=1}^K \mathbf{w}_{j,i}^G. \quad (7)$$

Iteratively aggregating global and local models in a class-wise manner, cwFedAVG facilitates personalization. Evidently, the server necessitates knowledge of each client’s class distribution information $p_{i,j}$, or an appropriate approximation thereof. In the subsequent section, we elucidate our proposed methodology for enabling the server to estimate $p_{i,j}$.

4 Weight Distribution Regularization for Class Distribution Estimation

This section introduces Weight Distribution Regularizer (WDR), and we elucidate the rationale behind WDR and its necessity for accurate class distribution estimation.

4.1 Estimating Class Distribution from Class-specific Weight Vectors

One obvious way to share a client’s class distribution with the server is to send $\mathbf{p}_i = [p_{i,1}, p_{i,2}, \dots, p_{i,K}]$ to the server directly, which is not allowed for privacy concern. In this study, we instead estimate the class distribution by leveraging the information contained in the weights of a deep network. Let $\Theta_i = [\theta_{i,1}, \theta_{i,2}, \dots, \theta_{i,K}]$ denote the weights between the penultimate layer and the output layer of a deep network of the i -th client. Each element of Θ_i represents the weight vector connecting the neurons of the penultimate layer to a specific neuron in the output layer, where each neuron corresponds to one of the classes in the dataset. In this work, we call $\theta_{i,j}$ j -th ‘class-specific weight vector’ of client i .

Anand et al. (1993) demonstrated the correlation between the gradients of class-specific weight vectors and the class distribution of local datasets, thereby enabling the estimation of the class distribution from these gradients, as detailed in the theorem presented in their paper.

Theorem 2. *For a deep network classifier of client i , the squared norms of the gradients of the class-specific weight vectors satisfy the following approximate relationship (Anand et al., 1993):*

$$\frac{\mathbb{E} \|\nabla \mathcal{L}(\theta_{i,j})\|_2^2}{\mathbb{E} \|\nabla \mathcal{L}(\theta_{i,k})\|_2^2} \approx \frac{n_{i,j}^2}{n_{i,k}^2}. \quad (8)$$

From the theorem, one can infer that there exists a correlation between the class distribution and certain statistical characteristics of the weight parameters rather than the gradients. In fact, we observed the distribution of the L2-norms of class-specific weight vectors and found that it correlates with the class distribution. Therefore, we approximate $p_{i,j}$ as follows:

$$\tilde{p}_{i,j} = \frac{\|\theta_{i,j}\|_2}{\sum_{j=1}^K \|\theta_{i,j}\|_2}. \quad (9)$$

The red triangle points in Figure 2c illustrate there exists a positive correlation between $p_{i,j}$ and $\tilde{p}_{i,j}$ for one example client with CIFAR-10 practical setting. However, one can notice that although $\tilde{p}_{i,j}$ is correlated with $p_{i,j}$, $\tilde{\mathbf{p}}_i$ is quite different from \mathbf{p}_i . Even when the number of data samples belonging to the j -th class is zero or nearly zero, $\tilde{p}_{i,j}$ still exhibits a non-negligible value around 0.1 (the leftmost triangles). This inaccurate approximation could pose a problem when $\tilde{\mathbf{p}}_i$ is utilized for class-wise model aggregations of cwFedAVG. In the following subsection, we elucidate how to estimate the class distribution more accurately by applying our novel regularization technique.

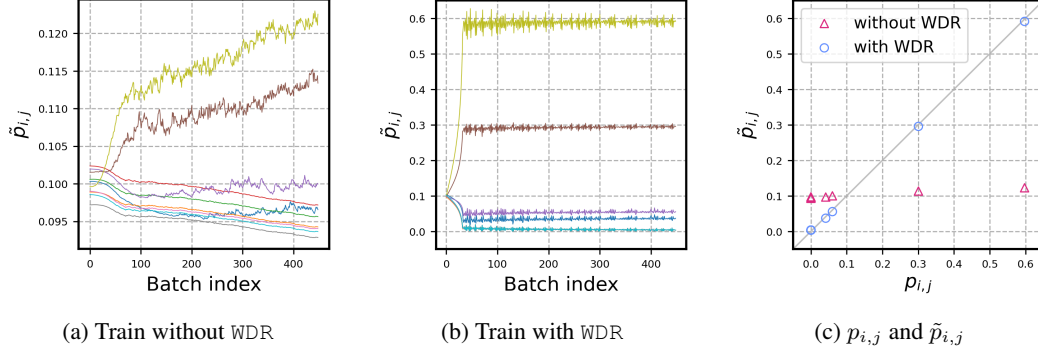


Figure 2: Visualizations of the influence of Weight Distribution Regularizer (WDR) for one example client of the CIFAR-10 practical setting. The line plots in (a) and (b) depict the evolution of the class distribution estimates, $\tilde{p}_{i,j}$, across mini-batch iterations during the first FL round. Each color corresponds to a different class. The scatter plot in (c) illustrates the relationship between the local class distribution, $p_{i,j}$, and their corresponding estimates, $\tilde{p}_{i,j}$, at the 449th mini-batch iteration.

4.2 Weight Distribution Regularizer

For \tilde{p}_i to become closer to p_i , we design WDR, which minimizes the Euclidean distance between p_i and \tilde{p}_i . It is defined as a penalty term $\Omega_i = \|p_i - \tilde{p}_i\|_2$, which is added to the original cost function \mathcal{L}_i . Then, the total cost function $\tilde{\mathcal{L}}_i$ can be denoted as $\tilde{\mathcal{L}}_i = \mathcal{L}_i + \lambda\Omega_i$, where $\lambda \in [0, \infty)$ is the penalty loss weight. We endeavor to find the largest possible value of λ with minimal accuracy loss by modulating λ . Figures 2a and 2b illustrate how $\tilde{p}_{i,j}$ evolves during mini-batches in a single round for one example client of the CIFAR-10 practical heterogeneous setting, without and with WDR, respectively. Each color corresponds to a different class. In this client, classes 0 and 1 are dominant, so $\tilde{p}_{i,0}$ and $\tilde{p}_{i,1}$ become more significant as batch iterations progress, as expected in both cases. However, without WDR, $\tilde{p}_{i,j}$ values are not well-separated, and all are around 0.1, which interferes with performing cwFedAVG properly. In contrast, with WDR, $\tilde{p}_{i,j}$ becomes more proximal to $p_{i,j}$.

cwFedAVG algorithm with WDR Algorithm 1 provides a comprehensive view of the federated learning process in cwFedAVG with WDR. The penalty loss weight λ can be an input parameter, and each client trains its local model with WDR, as described in line 7 of the algorithm. In practice, cwFedAVG could be performed with the true class distribution p_i without employing WDR, contingent upon the privacy level required for the specific application.

Algorithm 1: cwFedAVG with WDR

Input : M clients, penalty loss weight λ .

Output : The trained model parameter sets w_1^G, \dots, w_K^G and w_1^L, \dots, w_M^L .

- 1 $\forall j \in [K]$, randomly initialize global model $w_j^{G(0)}$ on the server.
 - 2 $\forall i \in [M]$, randomly initialize local model $w_i^{L(0)}$ on the clients.
 - 3 $\forall j \in [K]$ and $\forall i \in [M]$, initialize $\tilde{p}_{i,j}^{(0)}$ to $\frac{1}{K}$.
 - 4 **for** $r = 1, 2, \dots, R$ **do**
 - 5 Aggregate global models: the server computes $w_i^{L(r-1)}$ by weighted sum of $w_1^{G(r-1)}, \dots, w_K^{G(r-1)}$ with $\tilde{p}_{i,j}^{(r-1)}$ using Eq. (7).
 - 6 Download local models: each client downloads $w_i^{L(r-1)}$ from the server.
 - 7 Optimize local models: each client optimizes the downloaded model with WDR using λ .
 - 8 Upload local models: each client uploads $w_i^{L(r)}$ to the server.
 - 9 Aggregate local models: the server computes $\tilde{p}_{i,j}^{(r)}$ by Eq. (9) and $w_j^{G(r)}$ by weighted sum of $w_1^{L(r)}, \dots, w_M^{L(r)}$ using Eq. (3).
 - 10 **return** $w_1^{G(R)}, \dots, w_K^{G(R)}$ and $w_1^{L(R)}, \dots, w_M^{L(R)}$;
-

Setting	Pathological heterogeneous setting			Practical heterogeneous setting ($\beta = 0.1$)			
Method	MNIST	CIFAR-10	CIFAR-100	MNIST	CIFAR-10	CIFAR-100	AG News
FedAVG	98.08±0.11	60.68±0.84	28.22±0.32	98.70±0.04	61.94±0.56	32.44±0.42	79.57±0.17
FedProx	97.97±0.07	60.65±0.92	28.59±0.28	98.68±0.09	62.48±0.86	32.26±0.26	79.35±0.23
FedAMP	99.91±0.00	88.82±0.15	63.29±0.49	99.26±0.01	89.46±0.11	47.65±0.62	98.52±0.14
FedFomo	99.80±0.01	90.76±0.59	63.12±0.59	99.13±0.04	88.05±0.08	44.62±0.37	97.36±0.03
APPLE	99.75±0.03	90.21±0.21	63.12±0.12	99.49±0.33	90.57±0.24	54.92±0.43	96.00±0.11
CFL	98.02±0.04	60.58±0.15	28.55±0.30	98.70±0.00	61.40±0.51	44.19±0.69	33.89±1.78
IFCA	99.71±0.03	72.84±4.80	58.98±2.38	99.10±0.06	70.12±0.13	34.86±1.02	60.24±1.61
cwFedAVG w/ Dist.	99.86±0.02	91.35±0.22	67.37±0.31	99.52±0.03	89.53±0.10	48.27±0.74	98.37±0.04
cwFedAVG w/o WDR	97.94±0.07	61.29±0.09	28.67±0.91	98.71±0.05	62.72±0.34	32.25±0.56	74.24±0.39
cwFedAVG w/ WDR	99.87±0.02	<i>90.88±0.12</i>	<i>65.52±0.10</i>	99.47±0.03	89.54±0.15	55.38±0.10	98.43±0.04

Table 1: Accuracy performance (%). The ‘cwFedAVG w/ Dist.’ setting performs cwFedAVG without WDR, while model aggregations are based on the local class distribution of a client, p_i .

5 Experiments

In this section, we investigate the performance of cwFedAVG with four benchmark datasets for pathological and practical heterogeneous settings. Then, we present visualizations to demonstrate how effectively cwFedAVG with WDR personalizes local models.

5.1 Experimental Setup

We employ a 4-layer CNN with ReLU activation functions. No hyperparameter scheduler is incorporated to ensure a fair comparison. The learning rate of clients is set to 0.001, the batch size is 10, and the local training epochs are configured to 1, adhering to the configuration in (McMahan et al., 2017). The experimental setup comprises 20 clients, all participating in each round. The communication round is empirically set to 1,000 iterations to ensure convergence across all algorithms.

Four benchmark datasets—MNIST, CIFAR-10, CIFAR-100, and AG News—are employed to evaluate the proposed approach. Each dataset is subjected to pathological and practical heterogeneous settings. In the pathological setting, each client has data only from certain classes, while in the practical setting, client data distributions follow a Dirichlet distribution, mimicking non-uniform real-world data partitioning. We employ the highest mean testing accuracy achieved by an algorithm across all communication rounds during training as the evaluation metric, a widely adopted measure in the literature (T Dinh, Tran, and Nguyen, 2020). To establish a comprehensive baseline, we compare our method against seven algorithms spanning three distinct groups: (1) Traditional methods: FedAVG and FedProx; (2) Personalized aggregation-based methods: FedAMP, FedFomo and APPLE; (3) Clustering-based methods: CFL and IFCA. The reported results represent the average of three independent experiments conducted with different random seeds, ensuring statistical robustness. The code for the experiment was developed based on Zhang et al. (2023b)’s codebase, and the details of the experimental setup, such as the hardware and software configurations, are presented in the supplementary materials.

5.2 Performance Comparison and Analysis

Accuracy Table 1 illustrates that no single method consistently outperforms all others. However, in pathological and practical heterogeneous settings, PFL methods frequently outperform traditional FL methods such as FedAVG and FedProx. Among the PFL methods, cwFedAVG with different conditions typically ranks in the top 1 or 2 positions. Interestingly, the performance of cwFedAVG with WDR is comparable to cwFedAVG with Dist., which does not utilize WDR and use the local class distribution for aggregating models, indicating that WDR operates as designed. When excluding cwFedAVG with Dist., it is evident that cwFedAVG with WDR exhibits the best performance in four out of the seven evaluated settings (**bold** and *italic*). In the CIFAR-100 practical heterogeneous setting, cwFedAVG with WDR outperforms cwFedAVG with Dist., which is counter-intuitive. We observed that when the number of classes is significant in a practical heterogeneous setting, utilizing WDR and tuning the penalty loss weight (λ) accordingly can positively affect performance.

Experiment condition	Scalability				Heterogeneity		
	50 Clients		100 Clients		Dir ($\beta = 0.01$)	Dir ($\beta = 0.5$)	Dir ($\beta = 1.0$)
Setting	Acc. (%)	Time (s)	Acc. (%)	Time (s)	Acc. (%)	Acc. (%)	Acc. (%)
FedAVG	32.63±0.34	15.74	32.32±0.30	15.98	28.00±0.92	36.18±0.28	36.75±0.34
FedProx	33.22±0.20	17.79	32.64±0.21	18.40	27.89±0.24	35.93±0.31	36.65±0.39
FedAMP	44.97±0.27	19.16	41.37±0.35	25.55	73.46±0.40	25.41±0.14	21.23±0.40
FedFomo	42.62±0.62	42.16	38.62±0.08	46.36	71.30±0.03	25.43±0.58	18.95±0.34
APPLE	55.60±0.92	140.34	54.78±0.01	266.50	72.51±0.51	41.60±0.43	37.88±0.17
CFL	32.83±0.78	18.77	32.88±0.23	18.06	27.67±0.17	38.32±0.47	36.80±0.07
IFCA	29.17±0.44	127.23	26.56±0.45	198.92	53.89±3.58	25.87±0.57	22.27±1.14
cwFedAVG w/ Dist.	46.19±0.21	18.75	43.87±0.24	22.34	72.54±0.29	37.59±0.29	36.98±0.33
cwFedAVG w/o WDR	32.89±0.63	19.03	32.58±0.63	22.61	28.10±0.34	36.11±0.41	36.71±0.36
cwFedAVG w/ WDR	55.90±0.35	20.34	53.54±0.79	24.06	72.76±0.52	39.63±0.38	37.02±0.10

Table 2: Accuracy performance (%) of varying number of clients and β parameter. The ‘cwFedAVG w/ Dist.’ setting performs cwFedAVG without WDR, while model aggregations are based on the local class distribution of a client, \mathbf{p}_i .

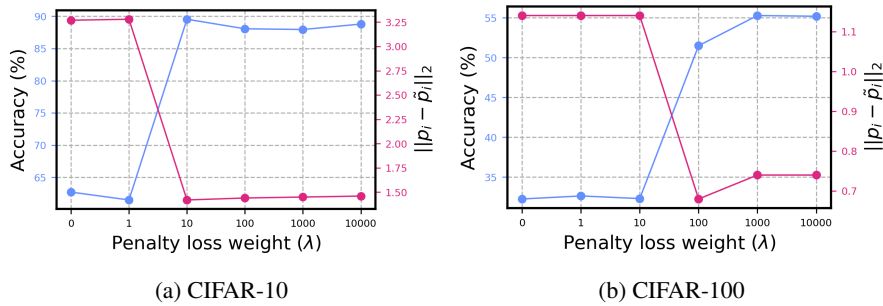


Figure 3: Visualizations of the penalty loss weight (λ)’s influence on accuracy and regularization term ($\|\mathbf{p}_i - \tilde{\mathbf{p}}_i\|_2$) for the CIFAR-10/100 practical heterogeneous settings.

Scalability To assess cwFedAVG algorithm’s scalability, we analyze the accuracy and computational overhead (time per round) with respect to the number of clients in a practical heterogeneous setting employing the CIFAR-100 dataset as shown in Table 2 (Left). As expected, the performance of all PFL methods degrades as the number of clients increases. However, cwFedAVG with WDR and APPLE exhibits greater robustness to the increasing number of clients compared to other PFL techniques. Regarding the computational overhead per round, cwFedAVG with WDR outperforms APPLE and other PFL methods, demonstrating its efficiency as it does not require any optimization process to learn optimal weights for combining clients or pairwise calculation. Furthermore, cwFedAVG has the same communication overhead as FedAVG because the class-wise local and global model aggregations are performed entirely on the server. However, a few PFL methods like APPLE download other clients’ local models from the server, which causes high communication costs and thus may be problematic when the number of clients exceeds a particular threshold.

Heterogeneity To analyze the sensitivity of cwFedAVG to data heterogeneity, we evaluate the accuracy under varying data distributions controlled by the β parameter of the Dirichlet distribution. As β increases, the heterogeneity of the local class distributions across clients decreases, implying that each client will have a similar amount of data for each class. The results in Table 2 (Right) demonstrate that only cwFedAVG with Dist., cwFedAVG with WDR, and APPLE exhibit robustness to changes in β . Furthermore, we observe that the performance of cwFedAVG with Dist. converges towards that of FedAVG as the β increases, which aligns with Theorem 1 presented in Section 3.

Effect of the penalty loss weight Figure 3 illustrates the impact of varying the penalty loss weight (λ) on the accuracy and the regularization term ($\|\mathbf{p}_i - \tilde{\mathbf{p}}_i\|_2$) for the CIFAR-10/100 practical heterogeneous settings. As anticipated, increasing λ leads to a decrease in the regularization term, as depicted in Figure 3. Based on this observation, we select the optimal λ value that maximizes the regularization strength while minimizing the accuracy degradation, as elaborated in Section 4.

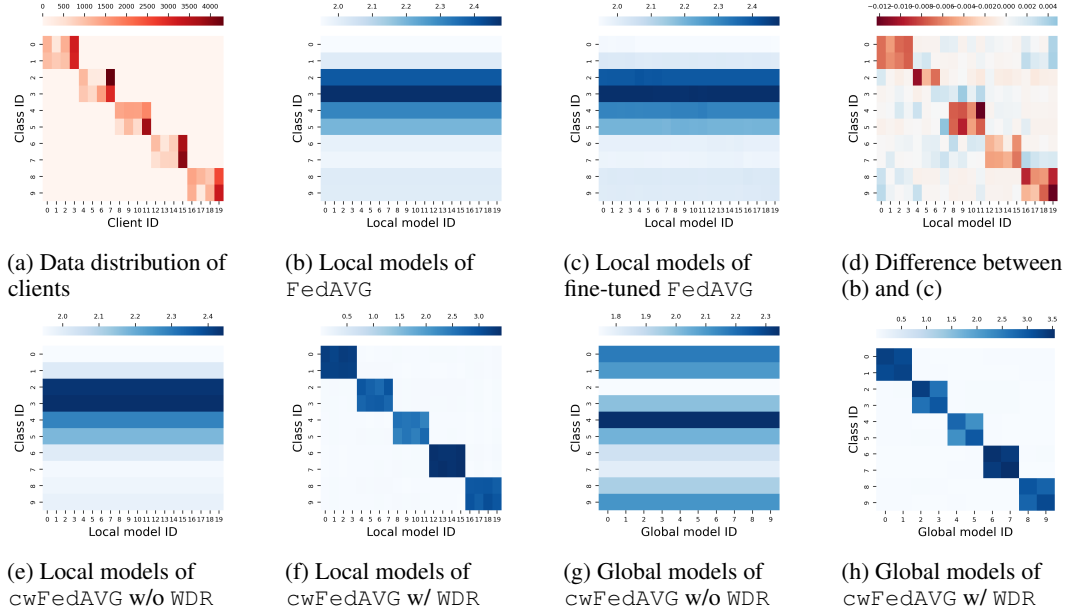


Figure 4: Heatmaps depicting the data distribution and L2-norms of class-specific weight vectors ($\|\theta_{i,j}\|_2$) for the CIFAR-10 pathological setting. (a) Each cell represents the number of data samples belonging to class j for client i . (b)-(h) Each cell shows $\|\theta_{i,j}\|_2$ of models for different FL methods.

5.3 Visualization of Personalized Models

To demonstrate how cwFedAVG achieves effective personalization of local models, we visualize heatmaps depicting the data distribution across clients and the norms of class-specific weight vectors ($\|\theta_{i,j}\|_2$) for local and global models, as shown in Figure 4. Figure 4a presents the number of samples for each class on 20 clients, illustrating the data distribution for the CIFAR-10 pathological setting. Next, Figures 4b and 4c do not show any distinctions between local models in contrast to Figure 4a and exhibit visually similar to each other. However, a closer inspection reveals subtle differences between the two at positions corresponding to the diagonal darker areas in Figure 4a. To highlight this distinction, Figure 4d visualizes the difference between the two heatmaps, where the diagonal areas appear darker, indicating that fine-tuned (personalized) local models can induce changes in the norms. Consequently, the norm can serve as a quantitative measure for assessing model personalization.

Notably, the heatmap of cwFedAVG without WDR (Figure 4e) closely resembles that of FedAVG (Figure 4b), aligning with the performance comparison in Table 1. In contrast, Figure 4f exhibits a pattern similar to Figure 4a, suggesting that each model has undergone personalization tailored to its possessed classes. Additionally, we visualize ten class-specific global models in Figures 4g and 4h. As designed and expected, each global model in Figure 4h specializes in specific classes since each client possesses data from only two classes in this setting—however, the models in Figure 4g do not. Visualizations for other datasets and settings are also provided in the supplementary materials.

6 Discussion and Conclusion

cwFedAVG requires handling multiple global models on the server equal to the number of classes. Thus, it may not perform well as designed for real-world applications where the number of classes is significantly larger than the number of data samples in each client since class distribution estimation can be unstable. However, our study has shown that cwFedAVG has distinct advantages over other algorithms in cross-device PFL scenarios. It eliminates the need for additional training on clients, pairwise information exchange between clients, or downloading other clients' models, which are typically required for other PFL methods. This not only simplifies the process but also enhances efficiency. Furthermore, as an aggregation module, cwFedAVG with WDR can be incorporated into other PFL methods to replace FedAVG, potentially leading to improved performance.

References

- Anand, R.; Mehrotra, K. G.; Mohan, C. K.; and Ranka, S. 1993. An improved algorithm for neural network classification of imbalanced training sets. *IEEE transactions on neural networks* 4(6):962–969.
- Briggs, C.; Fan, Z.; and Andras, P. 2020. Federated learning with hierarchical clustering of local updates to improve training on non-iid data. In *2020 International Joint Conference on Neural Networks (IJCNN)*, 1–9. IEEE.
- Choi, D., and Rhee, W. 2019. Utilizing class information for deep network representation shaping. In *Proceedings of the AAAI Conference on Artificial Intelligence*, volume 33, 3396–3403.
- Collins, L.; Hassani, H.; Mokhtari, A.; and Shakkottai, S. 2021. Exploiting shared representations for personalized federated learning. In *International conference on machine learning*, 2089–2099. PMLR.
- Duan, M.; Liu, D.; Ji, X.; Liu, R.; Liang, L.; Chen, X.; and Tan, Y. 2021. Fedgroup: Efficient federated learning via decomposed similarity-based clustering. In *2021 IEEE Intl Conf on Parallel & Distributed Processing with Applications, Big Data & Cloud Computing, Sustainable Computing & Communications, Social Computing & Networking (ISPA/BDCloud/SocialCom/SustainCom)*, 228–237. IEEE.
- Fallah, A.; Mokhtari, A.; and Ozdaglar, A. 2020. Personalized federated learning with theoretical guarantees: A model-agnostic meta-learning approach. *Advances in Neural Information Processing Systems* 33:3557–3568.
- Ghosh, A.; Chung, J.; Yin, D.; and Ramchandran, K. 2020. An efficient framework for clustered federated learning. *Advances in Neural Information Processing Systems* 33:19586–19597.
- Hsieh, K.; Phanishayee, A.; Mutlu, O.; and Gibbons, P. 2020. The non-iid data quagmire of decentralized machine learning. In *International Conference on Machine Learning*, 4387–4398. PMLR.
- Huang, Y.; Chu, L.; Zhou, Z.; Wang, L.; Liu, J.; Pei, J.; and Zhang, Y. 2021. Personalized cross-silo federated learning on non-iid data. In *Proceedings of the AAAI conference on artificial intelligence*, volume 35, 7865–7873.
- Johnson, J. M., and Khoshgoftaar, T. M. 2019. Survey on deep learning with class imbalance. *Journal of Big Data* 6(1):1–54.
- Kairouz, P.; McMahan, H. B.; Avent, B.; Bellet, A.; Bennis, M.; Bhagoji, A. N.; Bonawitz, K.; Charles, Z.; Cormode, G.; Cummings, R.; et al. 2021. Advances and open problems in federated learning. *Foundations and trends® in machine learning* 14(1–2):1–210.
- Li, T.; Sahu, A. K.; Zaheer, M.; Sanjabi, M.; Talwalkar, A.; and Smith, V. 2020. Federated optimization in heterogeneous networks. *Proceedings of Machine learning and systems* 2:429–450.
- Long, G.; Xie, M.; Shen, T.; Zhou, T.; Wang, X.; and Jiang, J. 2023. Multi-center federated learning: clients clustering for better personalization. *World Wide Web* 26(1):481–500.
- Luo, J., and Wu, S. 2022. Adapt to adaptation: Learning personalization for cross-silo federated learning. In *IJCAI: proceedings of the conference*, volume 2022, 2166. NIH Public Access.
- McMahan, B.; Moore, E.; Ramage, D.; Hampson, S.; and y Arcas, B. A. 2017. Communication-efficient learning of deep networks from decentralized data. In *Artificial intelligence and statistics*, 1273–1282. PMLR.
- Sattler, F.; Müller, K.-R.; and Samek, W. 2020. Clustered federated learning: Model-agnostic distributed multitask optimization under privacy constraints. *IEEE transactions on neural networks and learning systems* 32(8):3710–3722.
- T Dinh, C.; Tran, N.; and Nguyen, J. 2020. Personalized federated learning with moreau envelopes. *Advances in Neural Information Processing Systems* 33:21394–21405.

- Tan, A. Z.; Yu, H.; Cui, L.; and Yang, Q. 2022. Towards personalized federated learning. *IEEE Transactions on Neural Networks and Learning Systems*.
- Wang, L.; Xu, S.; Wang, X.; and Zhu, Q. 2021. Addressing class imbalance in federated learning. In *Proceedings of the AAAI Conference on Artificial Intelligence*, volume 35, 10165–10173.
- Yang, M.; Wang, X.; Zhu, H.; Wang, H.; and Qian, H. 2021. Federated learning with class imbalance reduction. In *2021 29th European Signal Processing Conference (EUSIPCO)*, 2174–2178. IEEE.
- Zhang, M.; Sapra, K.; Fidler, S.; Yeung, S.; and Alvarez, J. M. 2020. Personalized federated learning with first order model optimization. *arXiv preprint arXiv:2012.08565*.
- Zhang, J.; Li, Z.; Li, B.; Xu, J.; Wu, S.; Ding, S.; and Wu, C. 2022. Federated learning with label distribution skew via logits calibration. In *International Conference on Machine Learning*, 26311–26329. PMLR.
- Zhang, J.; Hua, Y.; Wang, H.; Song, T.; Xue, Z.; Ma, R.; and Guan, H. 2023a. Fedala: Adaptive local aggregation for personalized federated learning. In *Proceedings of the AAAI Conference on Artificial Intelligence*, volume 37, 11237–11244.
- Zhang, J.; Liu, Y.; Hua, Y.; Wang, H.; Song, T.; Xue, Z.; Ma, R.; and Cao, J. 2023b. Pflib: Personalized federated learning algorithm library. *arXiv preprint arXiv:2312.04992*.
- Zhao, Y.; Li, M.; Lai, L.; Suda, N.; Civin, D.; and Chandra, V. 2018. Federated learning with non-iid data. *arXiv preprint arXiv:1806.00582*.

Supplementary Materials

A Normalization Term for Class-wise Local Model Aggregation

In this section, we describe how the class-wise local model aggregation of cwFedAVG is analogous to the aggregation of FedAVG . FedAVG uses p_i to aggregate local models, considering only how much each local model contributes to updating the single global model. However, cwFedAVG should also consider $p_{i,j}$, the number of data samples for a specific class j on client i . The full derivation for the normalization term $q_{i,j}$ is as follows:

$$\mathbf{w}_j^G = \sum_{i=1}^M q_{i,j} \mathbf{w}_i^L \quad (10)$$

$$= \sum_{i=1}^M \frac{p_i \cdot p_{i,j}}{\sum_{i=1}^M p_i \cdot p_{i,j}} \mathbf{w}_i^L \quad (11)$$

$$= \sum_{i=1}^M \frac{\frac{n_i}{n} \cdot \frac{n_{i,j}}{n_i}}{\sum_{i=1}^M \frac{n_i}{n} \cdot \frac{n_{i,j}}{n_i}} \mathbf{w}_i^L \quad (12)$$

$$= \sum_{i=1}^M \frac{n_{i,j}}{\sum_{i=1}^M n_{i,j}} \mathbf{w}_i^L, \quad (13)$$

where $p_i = \frac{n_i}{n}$ and $p_{i,j} = \frac{n_{i,j}}{n_i}$.

B Proof of Theorem 1

The proof of Theorem 1 directly follows from Eq. (11) in the derivation presented in Section A of the supplementary materials. The theorem can be proved as follows:

Proof.

$$\mathbf{w}_j^G = \sum_{i=1}^M \frac{p_i \cdot p_{i,j}}{\sum_{i=1}^M p_i \cdot p_{i,j}} \mathbf{w}_i^L \quad (14)$$

$$= \sum_{i=1}^M \frac{\frac{n_i}{n} \cdot \frac{1}{K}}{\sum_{i=1}^M \frac{n_i}{n} \cdot \frac{1}{K}} \mathbf{w}_i^L \quad (15)$$

$$= \sum_{i=1}^M \frac{n_i}{n} \mathbf{w}_i^L \quad (16)$$

$$= \mathbf{w}^G, \quad (17)$$

where Eq. (15) follows from $p_{i,j} = \frac{1}{K}$ when the local class distribution of each client is uniform. \square

C Experimental Details

Datasets In our experimental setup, each dataset is partitioned into training and test sets, with 75% of the data allocated to the training set and the remaining 25% constituting the test set. For the pathological heterogeneous setting, the entire dataset is disjointly sampled based on the designated number of classes: 1) 2 classes: MNIST, CIFAR-10, AG News (2) 10 classes: CIFAR-100. In the practical heterogeneous setting, the data distribution across clients is sampled from a Dirichlet distribution controlled by the β parameter. This parameter governs the level of heterogeneity in the data distribution, with higher values of β corresponding to decreased heterogeneity, implying that

β	Heterogeneity (CIFAR-100)						
	Pathological	0.01	0.05	0.1	0.25	0.5	1.0
The number of classes with non-zero data	10	12	30	46	68	85	94

Table 3: The number of classes with non-zero data with different β parameters

Method	Hyperparameter settings
FedProx	μ (proximal term) = 0.001
FedAMP	α_k (gradient descent) = 1000, λ (regularization) = 1, σ (attention-inducing function) = 0.1
FedFomo	M (number of received local models) = the total number of clients
APPLE	η_2 (DR vector’s learning rate) = 0.01, μ (proximal term) = 0.1, L (loss scheduler) = 0.2
CFL	ϵ_1 (norm of averaged updated weight) = 0.4, ϵ_2 (norm of maximum updated weight) = 0.9
IFCA	k (number of clusters) = 4/2/8/2 for MNIST/CIFAR-10/CIFAR-100/AG News

Table 4: Hyperparameter settings for the baselines.

each client will have a similar proportion of data from each class. Table 3 shows The number of classes with non-zero data in the pathological heterogeneous setting and various values of β in the practical heterogeneous setting for CIFAR-100.

Hyperparameters Algorithm-specific hyperparameters for baselines such as μ (proximal term) in FedProx are chosen based on Zhang et al. (2023a), except for CFL and IFCA. Hyperparameters are set for CFL and IFCA, followed by their original papers. Details of hyperparameter settings for baselines are presented in Table 4.

Implementations The experiments are implemented using PyTorch 2.2 and conducted on a Google Cloud Platform (GCP) server with Intel Skylake CPUs (32 cores), 64GB memory, and four T4 GPUs running Ubuntu 20.04. The code for cwFedAVG is provided in the following GitHub repository: <https://github.com/regulation-sakak/cwFedAvg>.

D Visualizations of the Influence of Weight Distribution Regularizer for the CIFAR-100 Practical Heterogeneous Setting

In the CIFAR-100 practical heterogeneous setting, a similar pattern to the CIFAR-10 practical heterogeneous setting can be observed. For client ID 11, there are approximately ten dominant classes. Figure 5a demonstrates that the $\tilde{p}_{i,j}$ values of the dominant classes increase as the batch iterations progress. However, this increase is insufficient to resemble $p_{i,j}$. Thus, only a slight positive correlation can be observed in Figure 5c. With WDR, $\tilde{p}_{i,j}$ evolves like the CIFAR-10 practical heterogeneous setting (Figure 5b).

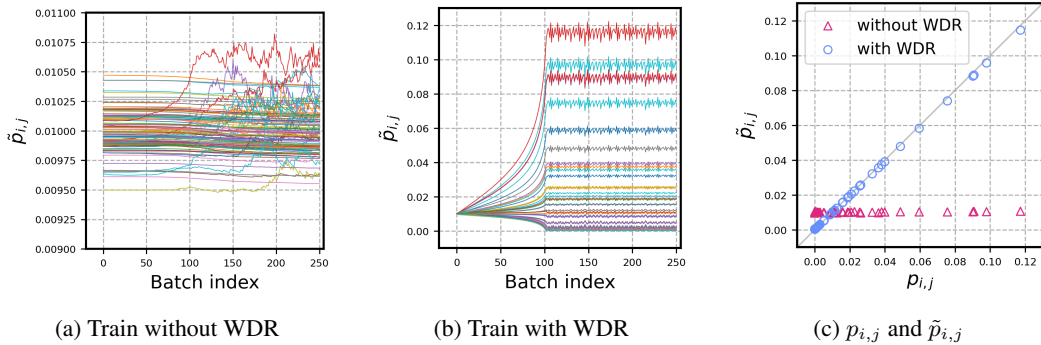


Figure 5: Visualizations of the influence of Weight Distribution Regularizer (WDR) for one example client of the CIFAR-100 practical heterogeneous setting.

E Visualizations of Clients' L2-norms of Class-specific Weight Vectors

This section explores the applicability of visualizing client L2-norms of class-specific weight vectors to the CIFAR-100 dataset, which has a significantly higher number of classes than CIFAR-10. Additionally, it examines whether the personalization patterns exhibited by the $cwFedAVG$ method, as depicted in Figure 4f, can be observed in other PFL algorithms such as FedAMP, FedFomo, and APPLE. Furthermore, the investigation aims to determine if clustering-based PFL approaches exhibit distinct patterns from the other methods under consideration.

E.1 CIFAR-100 Practical Heterogeneous Setting

Figure 6 confirms that the CIFAR-100 practical heterogeneous setting shows very similar patterns as the CIFAR-10 pathological heterogeneous setting.

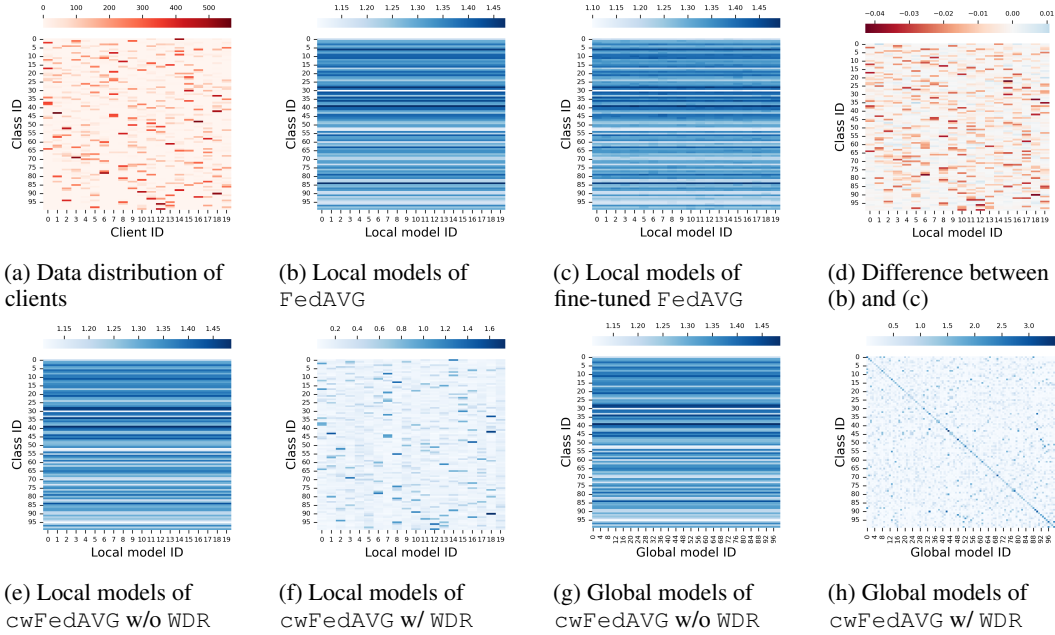


Figure 6: Heatmaps depicting the data distribution and L2-norms of class-specific weight vectors ($\|\theta_{i,j}\|_2$) for the CIFAR-100 practical heterogeneous setting. (a) Each cell represents the number of data samples belonging to class j for client i . (b)-(h) Each cell shows $\|\theta_{i,j}\|_2$ of models for different FL methods.

E.2 CIFAR-10 Practical Heterogeneous Setting

The CIFAR-10 practical heterogeneous setting confirms the observations from the CIFAR-10 pathological heterogeneous setting, as shown in Figure 7. Notably, PFL methods such as FedAMP and FedFomo exhibit patterns similar to the data distribution, albeit with less pronounced similarity compared to $cwFedAVG$. Despite APPLE's pattern not being visually discernible, a subtle pattern can be observed in Figure 7f, reminiscent of fine-tuned FedAVG in Figure 4c. Interestingly, clustering-based PFL methods, such as CFL and IFCA, exhibit distinct patterns, with two clusters evident in the heatmaps. Among the various FL and PFL approaches, $cwFedAVG$ demonstrates the most similar pattern with the true data distribution, suggesting its superior capability in personalizing clients.

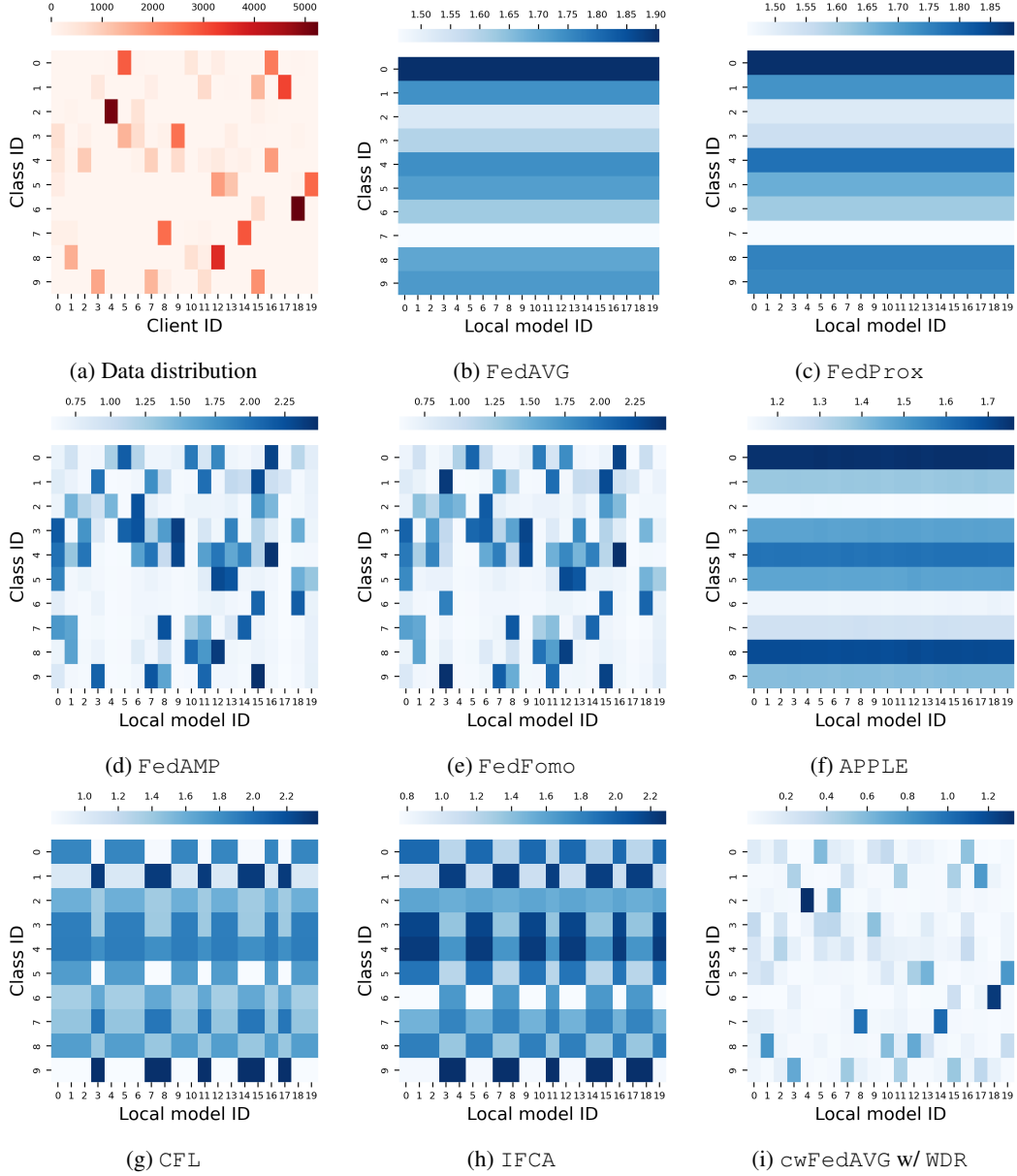


Figure 7: Heatmaps depicting the data distribution and L2-norms of class-specific weight vectors ($\|\theta_{i,j}\|_2$) for the CIFAR-10 practical heterogeneous setting. (a) Each cell represents the number of data samples belonging to class j for client i . (b)-(i) Each cell shows $\|\theta_{i,j}\|_2$ of models for different FL methods.